



Contents lists available at ScienceDirect

Journal of the Mechanical Behavior of Biomedical Materials

journal homepage: www.elsevier.com/locate/jmbbm

Collagen fibril tensile response described by a nonlinear Maxwell model

Martin Handelshauer^{a,b}, You-Rong Chiang^a, Martina Marchetti-Deschmann^b,
Philipp J. Thurner^a, Orestis G. Andriotis^{a,*}

^a Institute of Lightweight Design and Structural Biomechanics, TU Wien, 1060, Vienna, Austria^b Institute of Chemical Technologies and Analytics, TU Wien, 1060, Vienna, Austria

ARTICLE INFO

Keywords:

Nonlinear
Rheology
Collagen
Biomechanics
Soft tissues

ABSTRACT

Collagen fibrils are the basic structural building blocks that provide mechanical properties such as stiffness, toughness, and strength to tissues from the nano- to the macroscale. Collagen fibrils are highly hydrated and transient deformation mechanisms contribute to their mechanical behavior. One approach to describe and quantify the apparent viscoelastic behavior of collagen fibrils is to find rheological models and fit the resulting empirical equations to experimental data. In this study, we consider a nonlinear rheological Maxwell model for this purpose. The model was fitted to tensile stress-time data from experiments conducted in a previous study on hydrated and partially dehydrated individual collagen fibrils via AFM. The derivative tensile modulus, estimated from the empirical equation, increased for decreasing hydration of the collagen fibril. The viscosity is only marginally affected by hydration but shows a dependency with strain rate, suggesting thixotropic behavior for low strain rates.

1. Introduction

Collagens comprise a family of at least 28 different types of genetically distinct but closely related proteins (Myllyharju and Kivirikko, 2001). Constituting about 35% of the total human proteome, collagen, as a family, is one of the most abundant proteins in the human body (Smejkal and Fitzgerald, 2017). The most ubiquitous collagen, type I, self-assembles (copolymerizes with other fibril-forming collagens; II, III, V, XI, XXIV and XXVII) into supra-molecular rope-like architectures known as collagen fibrils (Sherman et al., 2015; Ottani et al., 2002; Kadler et al., 2007). Collagen fibrils are the basic structural building blocks of many biological tissues (tendon, ligaments, bone, cartilage, eye, etc.) providing structural and mechanical functions. In fact, collagen fibrils constitute most of the extracellular matrix (ECM) components, with which cells mechanically interact. This makes collagen fibrils interesting from a mechanobiological perspective and efforts to study their mechanical behavior play a pivotal role to gain further understanding of cell mechanotransduction.

Because of their high aspect ratio (lengths can be up to a few cm (Svensson et al., 2017; Craig et al., 1989), diameters range from 10 nm up to about 500 nm (Goh et al., 2005, 2008)) and their low flexural stiffness (Yang et al., 2007), collagen fibrils predominantly experience tensile loads *in vivo*. Mechanical characterization at the length scale of

individual and isolated collagen fibrils has been accomplished via tensile (Miyazaki and Hayashi, 1999; Van Der Rijt et al., 2006; Gentleman et al., 2003; Shen et al., 2008, 2011; Pins et al., 1997; Svensson et al., 2011, 2018; Andriotis et al., 2018; Silver et al., 2001), indentation (Andriotis et al., 2014, 2018; Wenger et al., 2007; Heim et al., 2006; Grant et al., 2008; Strasser et al., 2007) and bending tests (Yang et al., 2007). In tensile tests, commonly, a tensile modulus is estimated by derivation of a stress-strain curve in a linear region (Miyazaki and Hayashi, 1999; Van Der Rijt et al., 2006; Gentleman et al., 2003; Andriotis et al., 2018). For tendon fascicles, Svensson et al. derived a tensile modulus through a linear fit of the last 20 percent of the stress-strain curve (Svensson et al., 2011) and in their subsequent work on collagen fibrils calculated the first derivative of the stress-strain curve (Svensson et al., 2013, 2018). To make experimental data comparable, they proposed the detection of the first local maximum of tensile modulus-strain curves as a representative value (Svensson et al., 2013, 2018).

The mechanical behavior of hydrated collagen fibrils is far from being linear elastic and makes comparisons between studies challenging due to its complexity. Furthermore, it would be helpful for data analysis and modeling purposes to fit models to experimental data. However, collagen fibril mechanics are non-trivial, and several deformation mechanisms are often active at the same time. In the low strain regime investigated in this study, often classified as phase I (Svensson et al.,

* Corresponding author. Gumpendorfer Strasse 9, A-1060, Vienna, Austria.

E-mail address: orestis.andriotis@tuwien.ac.at (O.G. Andriotis).<https://doi.org/10.1016/j.jmbbm.2023.105991>

Received 25 November 2022; Received in revised form 20 June 2023; Accepted 23 June 2023

Available online 24 June 2023

1751-6161/© 2023 The Authors. Published by Elsevier Ltd. This is an open access article under the CC BY license (<http://creativecommons.org/licenses/by/4.0/>).

2013; Depalle et al., 2015), non-covalent interactions between molecules (Andriotis et al., 2018), the abundance of intrafibrillar water (both bound and unbound), the collagen molecule structure characterized by flexible kinks and unfolded regions along its length (Buehler and Wong, 2007), as well as covalent cross-links (Svensson et al., 2018) are responsible for the nonlinear and viscoelastic mechanical behavior of collagen fibrils under tension (Silver et al., 2001, 2002; Svensson et al., 2010; Gachon and Mesquida, 2020).

Different rheological models have been developed and employed in previous studies, to describe the mechanical behavior of collagen fibrils and collagen-rich tissues (macroscale). In this context, Shen et al., described the rheological behavior of collagen fibrils with a generalized Maxwell-Wiechert model in tensile stress relaxation tests employing a microelectromechanical system (MEMS) device (Shen et al., 2011). The model proposed by Shen et al. consists of two parallel Maxwell layers and an elastic spring, also in parallel. Based on this model, Shen et al. estimated the moduli of the three springs, including the time-independent modulus as well as the relaxation times, $\tau_{1,2}$, for the two Maxwell layers (Shen et al., 2011). Under quasistatic tension and at low strains (<5%), collagen fibrils show a nonlinear viscoelastic behavior (Van Der Rijt et al., 2006; Andriotis et al., 2018; Svensson et al., 2010; Yang et al., 2022). At strains less than 5%, stress increases exponentially (showing a convex shape similar to a toe region) which cannot be described using linear rheological models for viscoelastic solids or fluids. Also at higher strains, there is no true linear regime for hydrated fibrils (Svensson et al., 2013). Even though the Maxwell-Wiechert model described well the stress relaxation presented in the work by Shen et al., it was not an adequate choice for describing the viscoelastic behavior of collagen fibrils under quasistatic tension at low strains. Due to the convex shape of experimental stress-strain curves, a nonlinear rheological model may also be used to describe the mechanical behavior of collagen fibrils. The quasi-linear viscoelastic (QLV) model developed by Fung (1981) has been frequently used to describe the viscoelasticity of soft biological tissues (Johnson et al., 1994; Nekouzadeh et al., 2007; Kohandel et al., 2008). In Fung's theory the immediate non-linear elastic response and the linear viscous response, i.e., relaxation, are expressed in a reduced relaxation function. The set of parameters for the constitutive equation used in QLV, that could be eight or less, are estimated experimentally through a step change in strain (Kohandel et al., 2008). Thus, the QLV model and its extensions are applicable on strain-controlled experiments (i.e., stress relaxation tests) and instrument limitations may pose a barrier to applying this model, as is for example in most AFM-based tensile tests of individual and isolated collagen fibrils (Andriotis et al., 2023).

Because of these limitations, we investigated a nonlinear Maxwell model and sought out to describe the mechanical response of collagen

fibrils under continuous tension, as strain-controlled tests were not feasible with the instrument used (Andriotis et al., 2018). We tested the applicability of the model for describing the nonlinear viscoelastic behavior of collagen fibrils at small strains, that is up to about 2.5% engineering strain. We fitted the nonlinear Maxwell model on previously collected tensile data and compared it to a linear Maxwell model and a nonlinear spring. It should be noted, that the data of Andriotis et al. (2018) range within the deformation phase 1 (Fig. 1(a), strains up to 2.5%) and do not display the 2- or 3-phase behavior of collagen fibrils previously reported (Svensson et al., 2013).

2. Nonlinear maxwell model

The nonlinear Maxwell model consists of a nonlinear spring (spring constant a) and a nonlinear dashpot (viscosity μ) in series (see appendix). Under the assumption of a constant strain rate, i.e., $\epsilon(t) = kt$, the solution of the differential equation of the nonlinear Maxwell model leads to the equation for the time evolution of stress $\sigma(t)$:

$$\sigma(t) = k^{1/n} \mu \left(1 - e^{-t/\tau^n}\right)^{1/n}, \quad (1)$$

with time t [s], strain rate k [1/s], nonlinearity n and relaxation time $\tau = \frac{\mu}{a} [s^{1/n}]$. The influence of the exponent n is presented in Fig. 1(a) where the time evolution of stress is plotted for a constant strain rate and n to be equal to 0.15, 0.3, 0.6 to 1. For $n = 1$, the stress represents the linear Maxwell model as a boundary case. Substituting $t = \epsilon/k$ and calculating the first derivative of Eq. 1 with respect to strain gives the following simplified expression for the derivative tensile modulus as a function of strain:

$$E_{mod}(\epsilon) = \frac{\sigma(\epsilon)}{k n \tau^n} \left(e^{\frac{\epsilon}{\tau^n}} - 1\right)^{-1} \quad (2)$$

A more detailed derivation of the nonlinear Maxwell model is presented in Appendix A.

3. Materials and methods

3.1. Nanomechanical tensile tests and model fitting

We employed the nonlinear Maxwell model to a subset of previously collected experimental data published by Andriotis et al. (2018). Here, the stress vs. tensile tests performed at seven different displacement speeds in the range of 0.5–99.2 $\mu\text{m/s}$ and four solutions (phosphate buffered saline, 1.0M, 2.6M and 3.5M polyethylene glycol) were used. The experimental setup and methods are described by Andriotis et al. (2018). In brief, collagen fibrils were collected from a mouse-tail tendon and suspended between a cantilever of an atomic force microscope

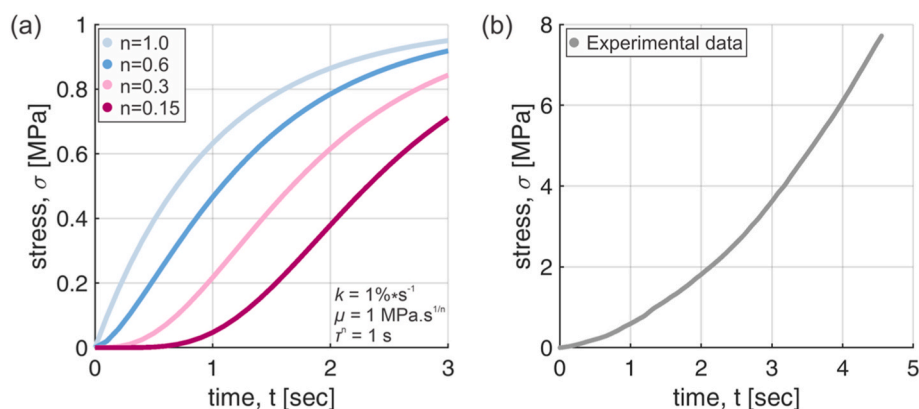


Fig. 1. (a) The influence of the exponent n on the resulting stress $\sigma(t)$. For $n = 1$, the model, i.e., Eq. 1, takes the form of the linear Maxwell model, resulting in an exponential increase of stress (with time or strain) until it plateaus. For $n < 1$ the resulting stress vs. time (or strain) takes a convex shape, which better describes the tensile response of collagen fibrils. (b) Exemplary stress vs. time data for a collagen fibril pulled at a displacement speed of 0.5 $\mu\text{m/s}$.

(AFM) and a glass slide using epoxy glue, similarly to (Svensson et al., 2010). Suspended collagen fibrils were mechanically tested by driving the AFM-cantilever upwards at seven different displacement speeds, which results in tensile stretch of the individual collagen fibrils. Collagen fibrils were stretched up to a maximum of about 2.5% engineering strain, which is well below failure, previously observed to occur above 10% Fig. 1(b)). Due to the inherent limitations of the instrument, only the displacement speed of the piezo crystal that drives the cantilever can be controlled. Therefore, experiments with controlled strain rate are not possible. However, the difference between displacement speed of the piezo and displacement rate of the fibril reaches a maximum of 29.4%, which had only a minor influence on the measured results. The experiments were conducted on a collagen fibril in different aqueous solutions of phosphate buffered saline (PBS) and varying concentrations of polyethylene glycol (PEG) of 0.1M, 2.6M and 3.5M. PEG was used as an agent to partially dehydrate the fibrils resulting into stiffening, observable in the recorded force-displacement but also calculated stress-strain curves (Andriotis et al., 2018). For these experiments one collagen fibril was tested, and in total six repeated tests were conducted per displacement speed and solution.

The recorded force-displacement data was converted into engineering stress and engineering strain (linear strain approximation) respectively. Data analysis was implemented in MATLAB R2019b (Version 9.7.0.1190202, The MathWorks, Inc., Natick, Massachusetts, USA). A curve-fit was performed using the least-squares method on the strain vs. time data, to determine the average fibril strain rate of the test. For the nonlinear models, we assumed a constant strain rate (which was set to the average strain rate) and hence the solutions provided in Equation 1 and 2). Subsequently, starting values were identified for the fitting parameters μ , τ and n , using an algorithm to randomize 100 different values for each fitting parameter and conducting each fit. The resulting R^2 values for the fits conducted using the randomized starting values were compared. The values of μ , τ and n returning the highest R^2 were considered as appropriate and used for further analysis. Overall, the fitting parameters, μ and τ were chosen to lie $(0, \infty)$, and the nonlinearity n within $(0, 1)$.

3.2. Statistics

The data, i.e., viscosity, relaxation time and exponent n , was subjected to statistical analysis using RStudio Version 2022.02.0. Individual value plots were used to visually inspect the data distribution, variability, and outliers. Generalized Least Squares was used to fit a linear model. Heteroscedasticity was accounted for in the model by allowing different variances per solution and speed. The model assumptions (normality, homoscedasticity) were inspected via the residual plots. The significance level was defined as $p < 0.05$, and p-values $p > 0.05$ but < 0.07 were considered tendencies. Tukey's test was used to correct for

multiplicity adjustment. All comparisons (either per solution or per displacement speed) and their p-value are provided as supplementary material.

4. Results

4.1. Comparison of linear and nonlinear models

The nonlinearity exponent, n , prominently influences the shape of the stress-time function and the quality of the fit. For $n = 1$, Equation 1 takes the form of the linear Maxwell model, which is qualitatively different to the experimentally determined mechanical behavior of individual collagen fibrils as shown in Fig. 2a. In the linear case, the Maxwell model, is not a convex function and therefore the fit for $n = 1$ returns a linear elastic response. Decreasing n to 0.6 and below, the Equation 1 turns into a convex function (Fig. 1(a)), which is qualitatively similar to the data obtained from experiments. Fig. 2(a) shows the fitting of a linear and nonlinear ($n = 0.6$) Maxwell model to experimental data. Here, the nonlinear model fits the data well whereas the linear model essentially returns the response of a linear spring and dashpot in series.

The derivative tensile modulus of the nonlinear Maxwell model is strain-dependent. In contrast, the linear Maxwell model yields a constant derivative tensile modulus and in this case is not a suitable choice for a fit function. Fig. 2(b) shows the derivative tensile modulus determined from the nonlinear Maxwell model ($n = 0.6$) fitted to the experimental data as a function of strain for different PEG concentrations.

4.2. Analysis of the nonlinear maxwell model

Equation 1 depends on the constants of the non-linear rheological elements, i.e., the exponent n and the (constant) strain rate, $de(t)/dt$ (cf. 2. Nonlinear Maxwell model). Consequently, the model consists of three parameters describing the viscous and elastic properties, and the nonlinearity. We first analyzed results from fitting all three parameters to experimental data obtained from tensile tests of individual collagen fibrils per displacement speed and per solution. In a second step, we set the exponent n to 0.6, as detailed below, to investigate the influence of lowering the number of fitting parameters on the results obtained from the nonlinear Maxwell model.

For all analyses the derivative tensile modulus was calculated using Equation 2. As shown in table S1.1, the values for the exponent n , when used as a free fitting parameter, were around 0.6 (0.56 ± 0.05 ; mean \pm standard deviation). Thus, we fixed the exponent n to a value of 0.6 for further analysis to reduce the number of fitting parameters. In Fig. 2(b), the derivative tensile modulus is plotted against strain for increasing displacement speeds (with $n = 0.6$). The derivative tensile modulus of

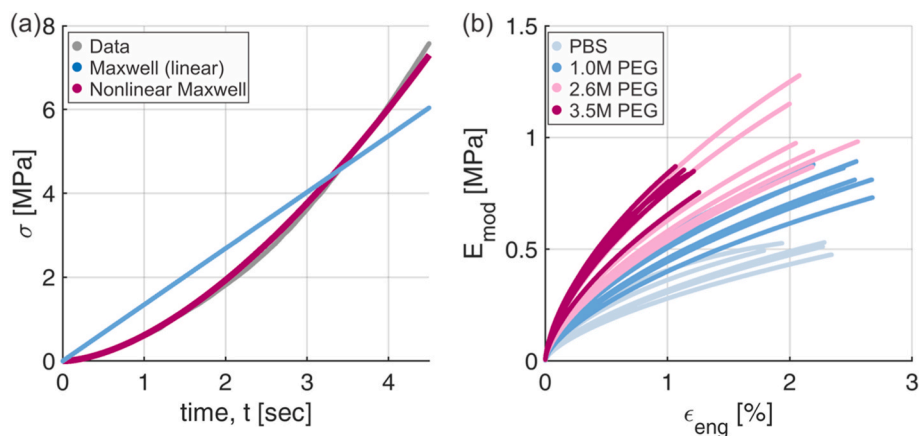


Fig. 2. (a) Fitting of the linear (red) and nonlinear Maxwell (blue) models to stress vs. time data from a tensile experiment on an individual collagen fibril measured in phosphate buffered saline (PBS). The fitting parameter n was fixed at 0.6 (based on the n that resulted to the best R^2). The nonlinear Maxwell model qualitatively and quantitatively fits the data whereas this is not the case for the linear model. (b) Derivative tensile modulus vs. strain at different PEG concentrations (i.e. water content reduces with increasing PEG concentration) obtained from fitting the nonlinear Maxwell model (Equation 2, $n = 0.6$) to the experimental data. The derivative tensile modulus rises with increasing PEG concentration. The experimental data used were collected at a displacement speed of $0.5 \mu\text{m/s}$.

the hydrated collagen fibril in PBS and at different PEG concentrations (Fig. 3) rises with strain and displacement speed. Furthermore, the absolute difference in derivative tensile modulus at different displacement speed is related to the PEG concentration. That is, the difference in derivative tensile modulus at 2.6M or 3M PEG between the lowest and highest displacement speeds is larger compared to PBS and 1M PEG. The increase of the derivative tensile modulus with strain rate is more prominent in the case of exposing the collagen fibril to 2.6M PEG (Fig. 3(c)).

The dataset, presented in Fig. 3, was also analyzed without fixing the exponent n , and instead using it as a third fit parameter. Fig. 4 shows the influence the displacement speed has on the derivative tensile moduli in this case. Similarly in Fig. 3, the absolute spread of the derivative tensile moduli at 2.6M and 3.5M PEG concentration (Fig. 4(c)), larger in comparison to a PEG concentration of 1.0M or PBS.

Overall, the influence of a free exponent n on the fitting shows a similar behavior of the derivative tensile modulus with that for a fixed exponent ($n = 0.6$). The goodness of fit R^2 , is slightly lower for a fixed compared to a free exponent n . Derivative tensile modulus determined from the nonlinear Maxwell model with a fixed exponent n show higher variation compared to ones obtained from fitting also n .

Clearly, the implementation of the exponent n as a third fitting parameter provides a larger parameter space for the fitting algorithm. This also decreases the variation for the derivative tensile moduli. Qualitative changes in the shape of the derivative tensile modulus functions are seen at 2.6M and 3.5M PEG for the highest displacement speeds (cf. Fig. 4(c) and (d)), which is not evident from the derivative tensile modulus obtained directly from the data (Andriotis et al., 2018). Therefore, we chose to fix n to 0.6.

Both the viscosity, μ , and relaxation time, τ , (for $n = 0.6$) decreased with increasing displacement speed for all solutions but most notable for PBS (cf. Figs. 5a and 6c; $p < 0.05$). However, differences in the relaxation time, τ^n [s], between the different solutions were not consistent and no clear trend was observed.

For the results with n as a fitting parameter, the viscosity measured in 2.6M PEG and at $0.5 \mu\text{m/s}$ was statistically significant different (cf. Fig. 5b; $p < 0.05$) to the ones measured at speeds $>1.3 \mu\text{m/s}$. However, there seems to be no trend of the viscosity with displacement speed. At lower displacement speeds ($0.5 \mu\text{m/s}$ to $12.4 \mu\text{m/s}$), statistically significant differences are observed in viscosity measured in PBS and 1.0M PEG compared to higher PEG concentrations. At higher speeds, the trend is not consistent.

For fitted n (cf. Fig. 6d), the relaxation time measured at PBS and 1.0M PEG is statistically different to the higher concentrations of PEG across all displacement speeds ($p < 0.05$).

In contrast to viscosity μ , and relaxation time τ^n [s], the spring constant, a [MPa], increased alongside the PEG concentration (cf. Fig. 6a; $p < 0.001$), while statistically significant differences were observed between lower ($<6.2 \mu\text{m/s}$) and higher ($>12.4 \mu\text{m/s}$) displacement speeds for $n=0.6$ (cf. Fig. 6a, $p < 0.05$). The spring constant obtained with n as a fitting parameter, showed a less consistent pattern, except the data obtained at 3.5M PEG, where the spring constant obtained at speeds $<1.3 \mu\text{m/s}$ are statistically different to the ones at displacement speeds $>6.2 \mu\text{m/s}$ (cf. Fig. 6b; $p < 0.001$).

5. Discussion

We employed a nonlinear Maxwell model to describe the mechanical

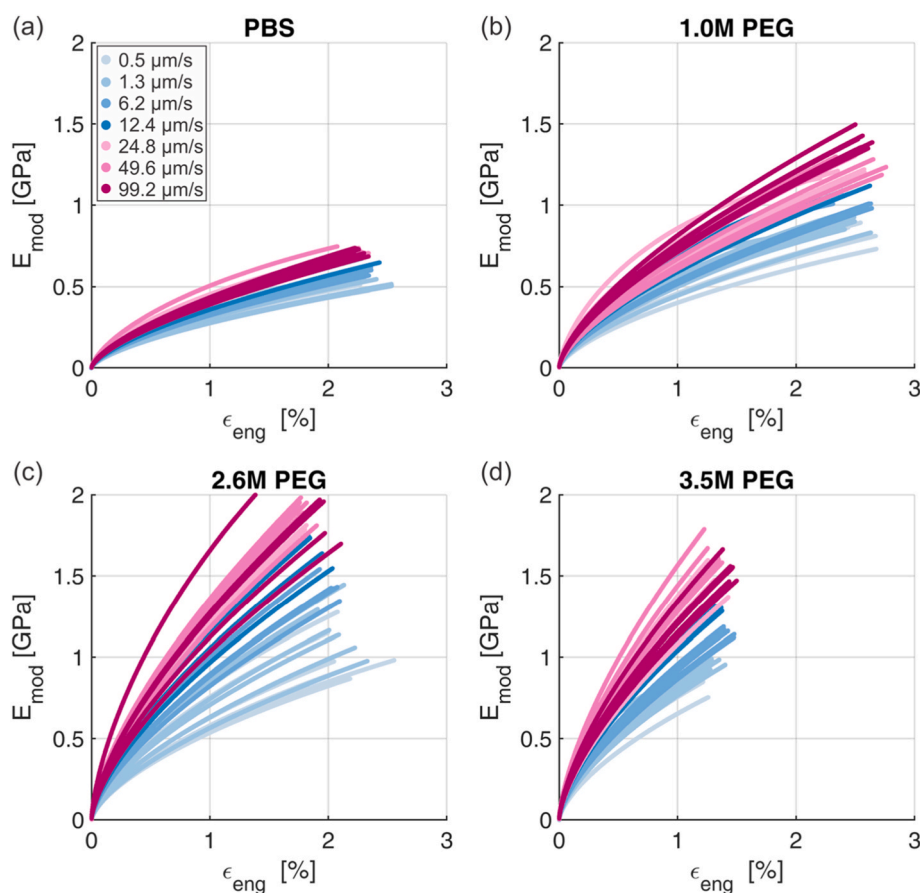


Fig. 3. Derivative tensile modulus vs. strain of a collagen fibril tested in four solutions with decreasing water content and at increasing displacement speeds. The derivative modulus was calculated from the nonlinear rheological Maxwell model (Equation (2)) for $n = 0.6$. The derivative tensile modulus increases nonlinearly with strain and is greater at a given strain for all different solutions. Also, the solution steers both of the aforementioned relationships.

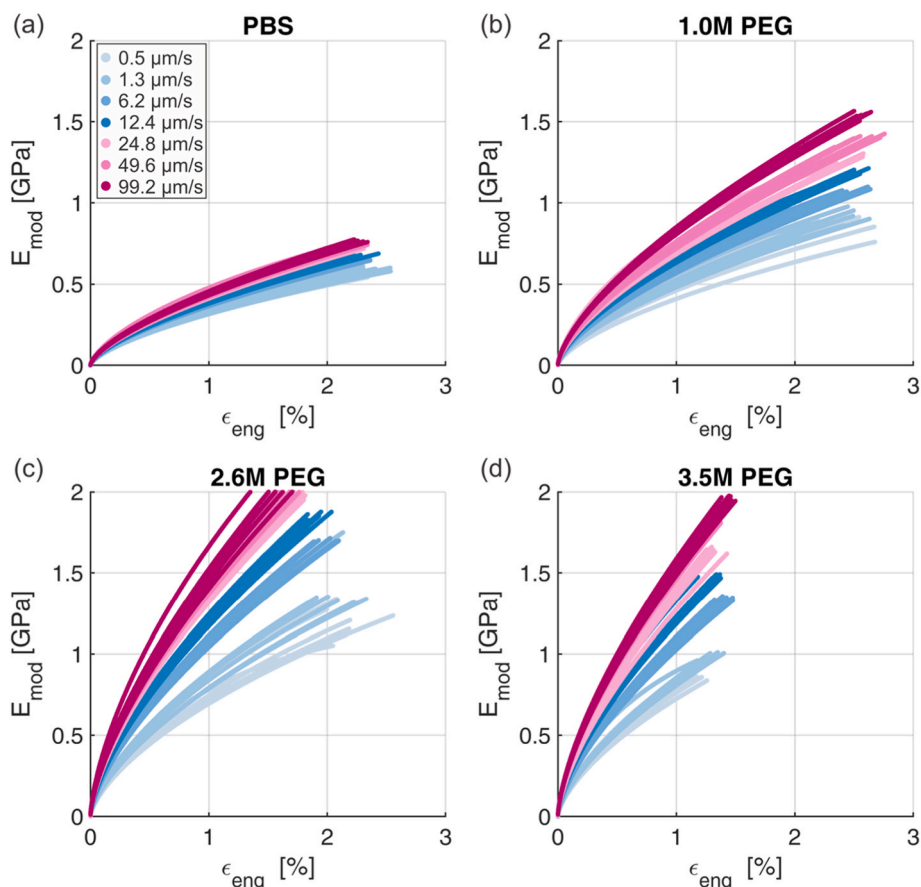


Fig. 4. Derivative tensile modulus vs. strain calculated from the nonlinear rheological Maxwell model (Equation (2)) using the exponent n as a fitting parameter. The derivative modulus increases similarly with displacement speed and solution (decreasing water content with increasing PEG concentration) is similar to the calculated derivative modulus with $n = 0.6$.

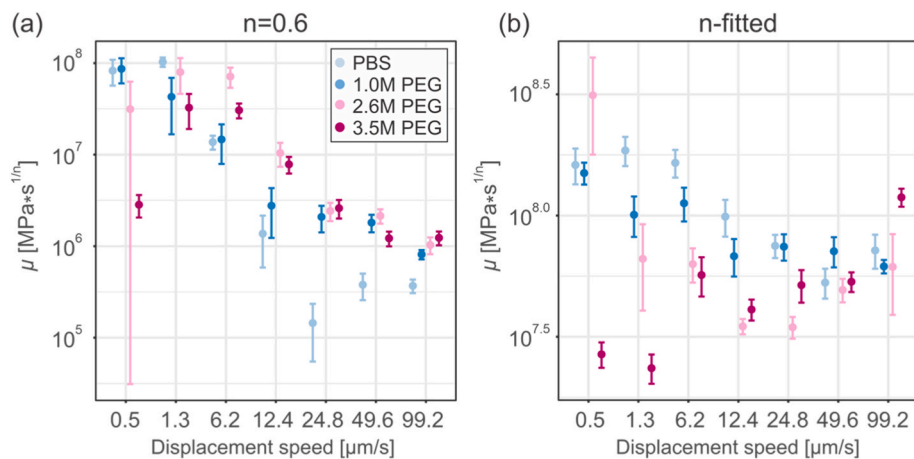


Fig. 5. Mean viscosity (\pm standard error of mean) vs. displacement speed for different solutions. Note that displacement speed data (x-axis) are not numerical but ordinal, hence the actual scale of the x-axis is not represented. (a) The viscosity for $n = 0.6$ decreased with increasing displacement speed. Here statistical significance was observed in viscosity measured (in PBS) at 0.5 $\mu\text{m/s}$, 1.3 $\mu\text{m/s}$, and 6.2 $\mu\text{m/s}$ compared to displacement speeds above 12.4 $\mu\text{m/s}$ ($p < 0.05$). (b) For n -fitted, the viscosity measured in 2.6M PEG and at 0.5 $\mu\text{m/s}$ was statistically significant different ($p < 0.05$) to the ones measured at speeds $>1.3 \mu\text{m/s}$, there seems to be no trend of the viscosity with displacement speed. However, at lower displacement speeds (0.5 $\mu\text{m/s}$ to 12.4 $\mu\text{m/s}$), statistically significant differences are observed in viscosity measured in PBS and 1.0M PEG compared to higher PEG concentrations. At higher speeds, the trend is not consistent.

behavior of a collagen fibril loaded in tension to small strains ($<1.5\%$), at different hydration levels and displacement speeds. Using the nonlinear Maxwell model, we determined the viscous and elastic properties, such as viscosity, elastic constant, and relaxation time as well as the derivative tensile modulus. At small strains ($<1.5\%$) the stress-strain curves of collagen fibrils generally show convex behavior. This regime differs from fibril to fibril and can extend to 7.5% strain (Svensson et al., 2013).

The derivative tensile modulus from the nonlinear Maxwell model presented here, reaches values of about 2 GPa which are in agreement

with results reported previously in studies investigating collagen fibrils under tension (Van Der Rijt et al., 2006; Shen et al., 2008; Svensson et al., 2018; Andriotis et al., 2018).

Hydration is well-known to affect the mechanical properties, i.e. stiffness, of individual collagen fibrils (Andriotis et al., 2015, 2018; Grant et al., 2008). The trend of increasing apparent tensile modulus of partially dehydrated collagen fibrils with increasing PEG concentration was also observed when we analyzed our experimental data with the nonlinear Maxwell model. This finding is in accordance with stress-strain data presented by Svensson et al. in an earlier study

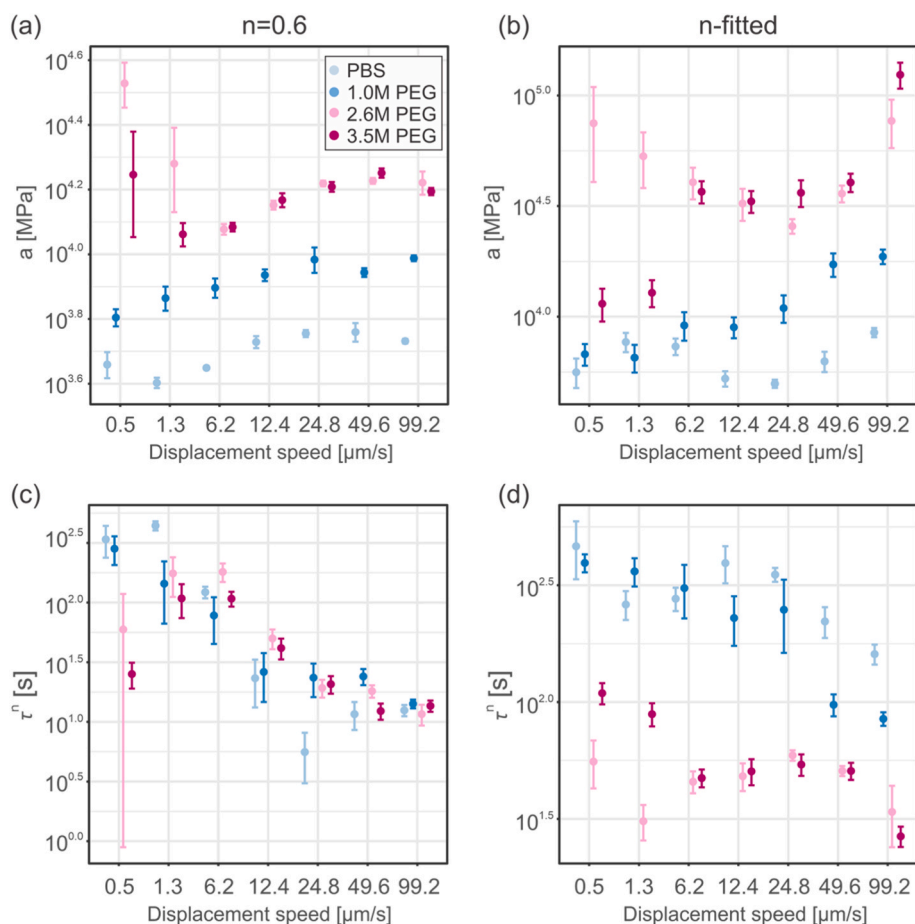


Fig. 6. (a, b) Mean spring constant and standard error of the mean plotted against the displacement speed for different PEG concentrations. The spring constant increases with PEG concentration, but the increase was significant only between lower ($<6.2 \mu\text{m/s}$) and higher ($<12.4 \mu\text{m/s}$) displacement speeds ($p < 0.05$). (c, d) Mean relaxation time τ^r [s] and standard error of the mean plotted against the displacement speed for different PEG concentrations. (c) For $n=0.6$, the relaxation time decreases with increasing displacement speed, but no clear trend was observed with PEG concentration. (d) For n -fitted, the relaxation time measured at PBS and 1.0M PEG is statistically different to the higher concentrations of PEG across all displacement speeds ($p < 0.05$).

(Svensson et al., 2010). We further find that the parameters of the rheological model are not constant but change either with displacement speed (i.e., fibril strain rate) or PEG concentration (i.e., hydration level). Interestingly, the elastic constant of the nonlinear spring, a , is predominantly affected by changes in PEG concentration, with higher stiffness for lower hydration levels. This reflects earlier interpretation (Andriotis et al., 2018), that the elastic behavior is in this case largely driven by the predominantly non-covalent interactions between the collagen molecules within the collagen fibril. With decreasing hydration, the content of intermolecular unbound water is reduced. Therefore, the interaction between neighboring molecules becomes stronger and leads to an increase in stiffness. In contrast, the viscosity is affected predominantly by the displacement speed, i.e., fibril strain rate. Viscous behavior of collagen fibrils has been previously linked to deformation mechanisms such as rupturing and forming of intramolecular hydrogen bonds (Gautieri et al., 2009, 2012). Intramolecular (i.e., collagen-collagen) hydrogen bonds, that stabilize the tropocollagen triple helix, rupture upon unwinding and straightening of the collagen triple helix while collagen-water hydrogen bonds are forming (Gautieri et al., 2009, 2011, 2012; Buehler, 2008). Bell formulated a simple theory on the formation and rupture of bonds between cells (Bell, 1978). Some of the concepts in Bell's theory could explain the origin of rate dependent mechanical properties in collagen fibrils. Bell showed that the applied force influences the rate at which hydrogen bonds rupture (Bell, 1978). According to Bell's model, if a steady and low force is applied hydrogen bonds rupture and reform reaching a new equilibrium. But if a larger force is applied at higher rate, hydrogen bonds will rupture rapidly (Bell, 1978).

Our data show that the applied force shifts to higher values while loading the collagen fibril at higher fibril strain rates at a given

concentration of PEG. Thus, loading at higher fibril strain rates allows less time for hydrogen bonds to reform and restabilize the collagen triple helix. This may explain the decreasing and plateauing viscosity in collagen fibrils with increasing strain rate. Our interpretation for this behavior is that when collagen-collagen hydrogen bonds rupture, collagen-water hydrogen bonds are forming. Driving the strain rate up, a point is reached where no more collagen-collagen and only collagen-water hydrogen bonds can form. This could explain the plateau region starting at a displacement speed of about $12 \mu\text{m/s}$, corresponding to a strain rate of about 0.122 s^{-1} .

The decrease of viscosity before reaching a plateau is about two orders of magnitude. This magnitude is in agreement with the study by Silver et al., who also reported a decrease of viscosity with strain-rate in tensile tests of self-assembled collagen fiber (Silver et al., 2002). But, the tests by Silver et al. were conducted on larger collagen fibers with diameters ranging between $38 \mu\text{m}$ to $70 \mu\text{m}$, whereas we extracted and tested individual collagen fibrils (Silver et al., 2002). Therefore, it is possible that some of the effects seen by Silver et al. stem from interactions of a collection of collagen fibrils composing a collagen fiber, rather than from individual collagen fibrils. In our study, the relaxation time, τ^r , decreases with increasing displacement speed, since τ^r is the ratio of the viscosity and the elastic constant of the nonlinear spring. To our knowledge only Shen et al. published values of the relaxation times using a Maxwell-Wiechert model (Shen et al., 2011). In the work by Shen et al., stress relaxation tests over a time span of about 100 s were conducted. A model with two viscosities was used, one for fast (tenths of seconds) and one for slow (hundreds of seconds) relaxation times (Shen et al., 2011). In contrast, we used a nonlinear Maxwell model, consisting of one nonlinear viscous element (and therefore relaxation time) to describe quasistatic tensile data. Regardless of the different model used,

we present relaxation times in the range of 0.2–500 s (lower values mostly represent the response of the collagen fibril at higher PEG concentration, while higher values correspond to lower PEG concentration or just PBS), of similar order of magnitude presented by Shen et al. (7 ± 2 s and 102 ± 5 s). However, there are also two fundamental differences between our tests and the ones reported by Shen et al. that need to be considered (Shen et al., 2011). These are a) the environment, in which the tests were carried out and b) the different loading protocols. We used data from tests of a collagen fibril fully submerged in aqueous solutions, while Shen et al. tested air-dried collagen fibrils. And, while we used data from monotonic tensile tests, Shen et al. carried out stress relaxation tests.

In summary, the nonlinear Maxwell model suggests that collagen fibrils viewed as a highly viscous fluid exhibiting thixotropic behavior, *i. e.*, decreasing viscosity with strain-rate up to a certain plateau. Because of the high viscosity, the tensile response of collagen fibrils is largely dominated by their elastic response. This suggests that a nonlinear spring might be a simpler and suitable model that could fit the data. For the sake of completeness, we also tried this approach. However, the nonlinear spring could only successfully be fitted to the data collected from tests conducted in PBS only. The derivative tensile modulus estimated from the nonlinear spring followed a similar trend with the one estimated from the nonlinear Maxwell model (Figure S1.2). Therefore, the nonlinear Maxwell model seems to be a sufficient extension of the nonlinear spring to fit the data and especially also account for the transient effect during tensile loading of the partially dehydrated collagen fibril.

Yang et al. recently (Yang et al., 2022) showed that the adaptive QLV (in contrast to the QLV of Fung (1981)) model adequately describes the nonlinear viscoelasticity of collagen fibrils. Lack of experimental capabilities to perform stress relaxation and creep experiments (Fung, 1981; Kohandel et al., 2008) in our setup did not facilitate a similar analysis as performed by Yang et al. (2022). Hence, our aim here was to employ a model that does not require stepwise tests (*i. e.*, stress relaxation or creep tests), and has a low number of fitting parameters.

Additionally, the application of the nonlinear model presented here to stress relaxation and/or creep tests could also be considered. Such studies warrant a further extension or choice of a different configuration, but this is beyond the scope of this study.

Clearly a potential limitation of the approach presented here is the sensitivity on the starting values for the fitting parameters. Different starting values may force the model to convergence to local minima and therefore underestimate or overestimate the model parameters. To avoid such effects, we initially tried to find those starting values (as described in the materials and methods) that yielded the highest R^2 . In addition, we acknowledge that, the sample size of six force curves per strain rate and PEG concentration is small. Nevertheless, given the complex nature of tensile tests on individual and isolated collagen fibrils most experiments published to date suffer from low throughput. A positive fact is that the experiments we rely on here were performed on the same collagen fibril, *i. e.*, different PEG concentrations, different displacement speeds. While this does not increase the number of samples it limits variability. We expect that collagen fibrils from the same source will behave similarly and therefore show the same effects presented albeit

considerable sample to sample variation.

In this context new development of dedicated instruments for testing individual collagen fibrils (Svensson et al., 2018; Nalbach et al., 2022) may aid in increasing the sample size in the future.

6. Conclusion

An empirical equation based on a nonlinear Maxwell model was derived to describe the apparent tensile elastic and viscous response of a collagen fibril tested in varying hydration levels and displacement speeds. The apparent tensile modulus (or derivative modulus) increases with decreasing hydration and with increasing displacement speed (for a given hydration level). On the other hand, viscosity and relaxation time seem to be independent of the hydration level, but both decrease with increasing displacement speed, reaching a plateau starting at about 12 $\mu\text{m/s}$ displacement speed. The latter suggests a thixotropic behavior for the tested collagen fibril. A possible underlying mechanism that can explain these observations is the influence of available intermolecular unbound water. The amount of intermolecular unbound water may steer the strength of intermolecular non-covalent interactions, while rupture and formation of collagen-collagen and collagen-water hydrogen bonds may explain the changes in viscosity due to increasing displacement speed.

CRedit authorship contribution statement

Martin Handelshauer: Writing – original draft, Methodology, Formal analysis. **You-Rong Chiang:** Data curation, Formal analysis, Writing – review & editing. **Martina Marchetti-Deschmann:** Supervision. **Philipp J. Thurner:** Writing – original draft, Validation, Supervision. **Orestis G. Andriotis:** Writing – original draft, Visualization, Validation, Supervision, Methodology, Investigation, Formal analysis, Writing – review & editing.

Declaration of competing interest

The authors declare that they have no known competing financial interests or personal relationships that could have appeared to influence the work reported in this paper.

Data availability

Data will be made available on request.

Acknowledgements

This work has partly been funded by the Vienna Science and Technology Fund (WWTF) [10.47379/LS19035]. Y.R. Chiang, P.J. Thurner and O.G. Andriotis would also like to acknowledge funding from the European Union's Horizon 2020 research and innovative programme under the Marie Skłodowska-Curie grant agreement No 101034277. The authors acknowledge TU Wien Bibliothek for financial support through its Open Access Funding Programme.

Appendix A. Supplementary data

Supplementary data to this article can be found online at <https://doi.org/10.1016/j.jmbbm.2023.105991>.

Appendix A

Nonlinear Maxwell model

Similar to the classical linear Maxwell model, the nonlinear Maxwell model consists of two elements, a dashpot, and a spring. The stress of the

spring and the dashpot in the nonlinear Maxwell model is a power law function, with exponent n , of the strain and strain rate, respectively ($\sigma_S(\varepsilon_S) = a\varepsilon_S^m, \sigma_D(\dot{\varepsilon}_D) = \mu \frac{d\varepsilon_D(t)}{dt}^{1/n}$, where a [Pa] the spring constant and μ [Pa • s^{1/n}] the viscosity). As shown in Fig. 1a, the exponent n influences how the stress increases with time or strain.

The nonlinear Maxwell model is described by the resulting differential equation (Khokhlov, 2016, 2019; Kobelev, 2014) by assuming $m = 1/n$.

$$\frac{d\varepsilon(t)}{dt} = \frac{n}{a^n} \sigma(t)^{n-1} \frac{d\sigma(t)}{dt} + \left(\frac{\sigma(t)}{\mu} \right)^n, \quad (A1)$$

with strain rate (constant in our case), $k = d\varepsilon(t)/dt$, assuming the initial condition $\varepsilon(t = 0) = 0$, stress $\sigma(t = 0) = 0$ and writing the relaxation time $\tau = \mu/a \left[\frac{s}{Pa} \right]$, the solution for equation (A1) is:

$$\sigma(t) = k^{1/n} \bullet \mu \bullet (1 - e^{-t/\tau^n})^{1/n}, \quad (A2)$$

Equation (A2) represents the evolution of stress vs. time, but we can also rewrite this equation as a function of strain (by substituting $t = \frac{\varepsilon}{k}$ [s], where ε the strain), and then calculate a derivative tensile modulus as a function of strain:

$$\sigma(\varepsilon) = k^{1/n} \bullet \mu \bullet (1 - e^{-\varepsilon/(k \tau^n)})^{1/n}$$

The derivative tensile modulus is:

$$\begin{aligned} E_{mod}(\varepsilon) &= \frac{d\sigma(\varepsilon)}{d\varepsilon} = \\ &= \frac{k^{-1+\frac{1}{n}} \bullet \mu \bullet e^{-\frac{\varepsilon}{k\tau^n}} (1 - e^{-\frac{\varepsilon}{k\tau^n}})^{-1+\frac{1}{n}}}{n \bullet \tau^n} = \\ &= \frac{k^{-1} \bullet \overbrace{k^{\frac{1}{n}} \bullet \mu \bullet (1 - e^{-\frac{\varepsilon}{k\tau^n}})^n}^{\sigma(\varepsilon)} \bullet e^{-\frac{\varepsilon}{k\tau^n}} \bullet (1 - e^{-\frac{\varepsilon}{k\tau^n}})^{-1}}{n \bullet \tau^n} \end{aligned}$$

Finally, the derivative tensile modulus takes the simplified form:

$$E_{mod}(\varepsilon) = \frac{\sigma(\varepsilon)}{k \bullet n \bullet \tau^n} (e^{\frac{\varepsilon}{k\tau^n}} - 1)^{-1}, \quad (A3)$$

References

- Andriotis, O.G., Manuyakorn, W., Zekonyte, J., Katsamenis, O.L., Fabri, S., Howarth, P. H., et al., 2014. Nanomechanical assessment of human and murine collagen fibrils via atomic force microscopy cantilever-based nanoindentation. *J. Mech. Behav. Biomed. Mater.* 39, 9–26. <https://doi.org/10.1016/j.jmbbm.2014.06.015> [Internet].
- Andriotis, O.G., Chang, S.W., Vanleene, M., Howarth, P.H., Davies, D.E., Shefelbine, S.J., et al., 2015. Structure-mechanics relationships of collagen fibrils in the osteogenesis imperfecta mouse model. *J. R. Soc., Interface* 12 (111).
- Andriotis, O.G., Desissaire, S., Thurner, P.J., 2018. Collagen fibrils: nature's highly tunable nonlinear springs. *ACS Nano* 12 (4), 3671–3680.
- Andriotis, O.G., Nalbach, M., Thurner, P.J., 2023. Mechanics of isolated individual collagen fibrils. *Acta Biomater.* 163, 35–49. <https://doi.org/10.1016/j.actbio.2022.12.008> [Internet].
- Bell, G.I., 1978. Models for the Specific Adhesion of Cells to Cells: a theoretical framework for adhesion mediated by reversible bonds between cell surface molecules. *Science* 200 (4342), 618–627, 80–.
- Buehler, M.J., 2008. Nanomechanics of collagen fibrils under varying cross-link densities: atomistic and continuum studies. *J. Mech. Behav. Biomed. Mater.* 1 (1), 59–67.
- Buehler, M.J., Wong, S.Y., 2007. Entropic elasticity controls nanomechanics of single tropocollagen molecules. *Biophys. J.* 93 (1), 37–43. <https://doi.org/10.1529/biophysj.106.102616> [Internet].
- Craig, A.S., Birtles, M.J., Conway, J.F., Parry, D.A.D., 1989. An estimate of the mean length of collagen fibrils in rat tail-tendon as a function of age. *Connect. Tissue Res.* 19 (1), 51–62 [Internet]. <http://www.tandfonline.com/doi/full/10.3109/03008208909016814>.
- Depalle, B., Qin, Z., Shefelbine, S.J., Buehler, M.J., 2015. Influence of cross-link structure, density and mechanical properties in the mesoscale deformation mechanisms of collagen fibrils. *J. Mech. Behav. Biomed. Mater.* 52, 1–13.
- Fung, Y.C., 1981. *Biomechanics: Mechanical Properties of Living Tissues*.
- Gachon, E., Mesquida, P., 2020. Stretching single collagen fibrils reveals nonlinear mechanical behavior. *Biophys. J.* 118 (6), 1401–1408. <https://doi.org/10.1016/j.bpj.2020.01.038> [Internet].
- Gautieri, A., Buehler, M.J., Redaelli, A., 2009. Deformation rate controls elasticity and unfolding pathway of single tropocollagen molecules. *J. Mech. Behav. Biomed. Mater.* 2 (2), 130–137. <https://doi.org/10.1016/j.jmbbm.2008.03.001> [Internet].
- Gautieri, A., Vesentini, S., Redaelli, A., Buehler, M.J., 2011. Hierarchical structure and nanomechanics of collagen microfibrils from the atomistic scale up. *Nano Lett.* 11 (2), 757–766.
- Gautieri, A., Vesentini, S., Redaelli, A., Buehler, M.J., 2012. Viscoelastic properties of model segments of collagen molecules. *Matrix Biol.* 31 (2), 141–149. <https://doi.org/10.1016/j.matbio.2011.11.005> [Internet].
- Gentleman, E., Lay, A.N., Dickerson, D.A., Nauman, E.A., Livesay, G.A., Dee, K.C., 2003. Mechanical characterization of collagen fibers and scaffolds for tissue engineering. *Biomaterials* 24 (21), 3805–3813.
- Goh, K.L., Hiller, J., Haston, J.L., Holmes, D.F., Kadler, K.E., Murdoch, A., et al., 2005. Analysis of collagen fibril diameter distribution in connective tissues using small-angle X-ray scattering. *Biochim. Biophys. Acta Gen. Subj.* 1722 (2), 183–188.
- Goh, K.L., Holmes, D.F., Lu, H.Y., Richardson, S., Kadler, K.E., Purslow, P.P., et al., 2008. Ageing changes in the tensile properties of tendons: influence of collagen fibril volume fraction. *J. Biomech. Eng.* 130 (2), 1–8.
- Grant, C.A., Brockwell, D.J., Radford, S.E., Thomson, N.H., 2008. Effects of hydration on the mechanical response of individual collagen fibrils. *Appl. Phys. Lett.* 92 (23).
- Heim, A.J., Matthews, W.G., Koob, T.J., 2006. Determination of the elastic modulus of native collagen fibrils via radial indentation. *Appl. Phys. Lett.* 89 (18).
- Johnson, G.A., Tramaglino, D.M., Levine, R.E., Ohno, K., Choi, N.-Y., Woo S, L.-Y., 1994. Tensile and viscoelastic properties of human patellar tendon. *J. Orthop. Res.* 12 (6), 796–803.
- Kadler, K.E., Baldock, C., Bella, J., Boot-Handford, R.P., 2007. Collagens at a glance. *J. Cell Sci.* 120 (12), 1955–1958.
- Khokhlov, A.V., 2016. Properties of a nonlinear viscoelastoplastic model of Maxwell type with two material functions. *Moscow Univ. Mech. Bull.* 71 (6), 132–136.
- Khokhlov, A.V., 2019. Applicability indicators and identification techniques for a nonlinear maxwell-type elastoviscoplastic model using loading-unloading curves. *Mech. Compos. Mater.* 55 (2), 195–210.
- Kobelev, V., 2014. Some basic solutions for nonlinear creep. *Int. J. Solid Struct.* 51 (19–20), 3372–3381. <https://doi.org/10.1016/j.ijsolstr.2014.05.029> [Internet].
- Kohandel, M., Sivaloganathan, S., Tenti, G., 2008. Estimation of the quasi-linear viscoelastic parameters using a genetic algorithm. *Math. Comput. Model.* 47 (3–4), 266–270.
- Miyazaki, H., Hayashi, K., 1999. Tensile tests of collagen fibers obtained from the rabbit patellar tendon. *Biomed. Microdevices* 2 (2), 151–157.
- Myllyharju, J., Kivirikko, K.I., 2001. Collagens and collagen-related diseases. *Ann. Med.* 33 (1), 7–21.
- Nalbach, M., Chalupa-Gantner, F., Spoerl, F., de Bar, V., Baumgartner, B., Andriotis, O. G., et al., 2022. Instrument for tensile testing of individual collagen fibrils with facile sample coupling and uncoupling. *Rev Sci Instrum* [Internet] 93 (5), 054103. <https://doi.org/10.1063/5.0072123>.

- Nekouzadeh, A., Pryse, K.M., Elson, E.L., Genin, G.M., 2007. A simplified approach to quasi-linear viscoelastic modeling. *J. Biomech.* 40 (14), 3070–3078 [Internet]. <https://linkinghub.elsevier.com/retrieve/pii/S0021929007001352>.
- Ottani, V., Martini, D., Franchi, M., Ruggeri, A., Raspanti, M., 2002. Hierarchical structures in fibrillar collagens. *Micron* 33 (7–8), 587–596.
- Pins, G.D., Huang, E.K., Christiansen, D.L., Silver, F.H., 1997. Effects of static axial strain on the tensile properties and failure mechanisms of self-assembled collagen fibers. *J. Appl. Polym. Sci.* 63 (11), 1429–1440.
- Shen, Z.L., Dodge, M.R., Kahn, H., Ballarini, R., Eppell, S.J., 2008. Stress-strain experiments on individual collagen fibrils. *Biophys J* [Internet] 95 (8), 3956–3963. <https://doi.org/10.1529/biophysj.107.124602>.
- Shen, Z.L., Kahn, H., Ballarini, R., Eppell, S.J., 2011. Viscoelastic properties of isolated collagen fibrils. *Biophys J* [Internet] 100 (12), 3008–3015. <https://doi.org/10.1016/j.bpj.2011.04.052>.
- Sherman, V.R., Yang, W., Meyers, M.A., 2015. The materials science of collagen. *J. Mech. Behav. Biomed. Mater.* 52, 22–50. <https://doi.org/10.1016/j.jmbbm.2015.05.023> [Internet].
- Silver, F.H., Christiansen, D.L., Snowhill, P.B., Chen, Y., 2001. Transition from viscous to elastic-based dependency of mechanical properties of self-assembled type I collagen fibers. *J. Appl. Polym. Sci.* 79 (1), 134–142.
- Silver, F.H., Ebrahimi, A., Snowhill, P.B., 2002. Viscoelastic properties of self-assembled type I collagen fibers: molecular basis of elastic and viscous behaviors. *Connect. Tissue Res.* 43 (4), 569–580.
- Smejkal, G.B., Fitzgerald, C., 2017. Revised estimate of total collagen in the human body. *Int J Proteomics Bioinforma* 2 (1), 1–2.
- Strasser, S., Zink, A., Janko, M., Heckl, W.M., Thalhammer, S., 2007. Structural investigations on native collagen type I fibrils using AFM. *Biochem. Biophys. Res. Commun.* 354 (1), 27–32.
- Svensson, R.B., Hassenkam, T., Hansen, P., Peter Magnusson, S., 2010. Viscoelastic behavior of discrete human collagen fibrils. *J Mech Behav Biomed Mater* [Internet] 3 (1), 112–115. <https://doi.org/10.1016/j.jmbbm.2009.01.005>.
- Svensson, R.B., Hassenkam, T., Hansen, P., Kjaer, M., Magnusson, S.P., 2011. Tensile force transmission in human patellar tendon fascicles is not mediated by glycosaminoglycans. *Connect. Tissue Res.* 52 (5), 415–421.
- Svensson, R.B., Mulder, H., Kovanen, V., Magnusson, S.P., 2013. Fracture mechanics of collagen fibrils: influence of natural cross-links. *Biophys J* [Internet] 104 (11), 2476–2484. <https://doi.org/10.1016/j.bpj.2013.04.033>.
- Svensson, R.B., Herchenhan, A., Starborg, T., Larsen, M., Kadler, K.E., Qvortrup, K., et al., 2017. Evidence of structurally continuous collagen fibrils in tendons. *Acta Biomater.* 50, 293–301. <https://doi.org/10.1016/j.actbio.2017.01.006> [Internet].
- Svensson, R.B., Smith, S.T., Moyer, P.J., Magnusson, S.P., 2018. Effects of maturation and advanced glycation on tensile mechanics of collagen fibrils from rat tail and Achilles tendons. *Acta Biomater.* 70, 270–280. <https://doi.org/10.1016/j.actbio.2018.02.005> [Internet].
- Van Der Rijt, J.A.J., Van Der Werf, K.O., Bennink, M.L., Dijkstra, P.J., Feijen, J., 2006. Micromechanical testing of individual collagen fibrils. *Macromol. Biosci.* 6 (9), 699–702.
- Wenger, M.P.E., Bozec, L., Horton, M.A., Mesquidaz, P., 2007. Mechanical properties of collagen fibrils. *Biophys. J.* 93 (4), 1255–1263. <https://doi.org/10.1529/biophysj.106.103192> [Internet].
- Yang, L., van der Werf, K.O., Koopman, B.F.J.M., Subramaniam, V., Bennink, M.L., Dijkstra, P.J., et al., 2007. Micromechanical bending of single collagen fibrils using atomic force microscopy. *J. Biomed. Mater. Res., Part A* 82A (1), 160–168.
- Yang, F., Das, D., Karunakaran, K., Genin, G.M., Thomopoulos, S., Chasiotis, I., 2022. Nonlinear time-dependent mechanical behavior of mammalian collagen fibrils. *Acta Biomater.*